

# MATERIALS CHEMISTRY

---

## FRONTIERS



CHINESE  
CHEMICAL  
SOCIETY



ROYAL SOCIETY  
OF CHEMISTRY

[rsc.li/frontiers-materials](https://rsc.li/frontiers-materials)

## RESEARCH ARTICLE

View Article Online  
View Journal | View Issue

Cite this: *Mater. Chem. Front.*,  
2023, 7, 4460

# Synthesis of composite imprinted polymer membranes for the selective removal of 17 $\beta$ -estradiol from water†

Zahra Niavarani,<sup>a</sup> Daniel Breite,<sup>a</sup> Andrea Prager,<sup>a</sup> Isabell Thomas,<sup>a</sup>  
Mathias Kuehnert,<sup>a</sup> Bernd Abel,<sup>b</sup> Roger Gläser<sup>id</sup><sup>b</sup> and Agnes Schulze<sup>id</sup>\*<sup>a</sup>

Composite microfiltration polyethersulfone membranes incorporating molecularly imprinted particles (MIPs) were developed for efficient and selective adsorption of 17 $\beta$ -estradiol from water. MIP particles were synthesized via precipitation polymerization, with 17 $\beta$ -estradiol as the template molecule. The composite membranes were prepared by embedding the MIPs into the membrane matrices using phase inversion process. Electron beam irradiation was used to covalently immobilize the MIP particles within the membrane scaffold. The synthesized membranes were characterized using scanning electron microscopy (SEM), X-ray photoelectron spectroscopy (XPS), water contact angle analysis, permeation tests and mercury porosimetry. The adsorption loading, selectivity, reusability, and adsorption isotherms were studied through batch and dynamic adsorption experiments. The results indicated significant adsorption loading of 17 $\beta$ -estradiol ( $12.9 \pm 1 \text{ mg g}^{-1}$ ) and selectivity factors as high as 6.2 and 12.5 for 17 $\beta$ -estradiol in the presence of model micropollutants (such as bisphenol A and citalopram), respectively. Moreover, the composite membranes were regenerated and reused without any significant loss in adsorption loading for 10 subsequent cycles. The maximum adsorption capacity of 17 $\beta$ -estradiol on the composite membrane, calculated by fitting experimental data with the Langmuir equation, was  $21.9 \text{ mg g}^{-1}$ , which is more than a 200-fold increase in the adsorption loading compared to commercial nanofiltration. These composite microfiltration membranes exhibit a high adsorption loading accompanied by lower pressure requirements for filtration, high water permeation, and extended reusability, rendering them a viable and sustainable option for water purification processes.

Received 3rd April 2023,  
Accepted 12th July 2023

DOI: 10.1039/d3qm00345k

rsc.li/frontiers-materials

## Introduction

The increasing contamination of freshwater resources and wastewaters as a result of industrial activity has become a serious environmental problem.<sup>1</sup> One class of contaminating compounds consists of endocrine disrupting compounds (EDCs), which pose a serious health threat to humans, mammals, and aquatic life.<sup>2</sup> 17 $\beta$ -estradiol (E2), the primary female sex hormone, is one of the most potent forms of estrogenic EDCs. Increasing levels of synthetic and natural E2 have been detected in natural water bodies around the world due to natural human activities.<sup>3</sup> Exposure to even trace concentrations of E2 ( $\mu\text{g L}^{-1}$  to  $\text{ng L}^{-1}$ ) can be a major risk for different

types of cancer.<sup>4</sup> Thus, developing efficient methods to remove E2 from aqueous media is in great demand. Among various conventional and advanced treatment methods to remove E2, adsorption on activated carbon (AC) and graphene oxide (GO) has attracted much attention due to their high removal capacity.<sup>5</sup> However, these adsorbents are often not specific and sustainable. Despite the low cost and availability of the AC, the on-site regeneration techniques are missing. AC has to be transported long distances (typically more than 100 km) to high temperature ( $> 800 \text{ }^{\circ}\text{C}$ ) facilities. Moreover, the thermal regeneration adds substantially to the CO<sub>2</sub> emissions. In addition, reduction of adsorption capacities after a few cycles have been reported due to loss of surface functional groups. GO and GO-immobilized membranes have not yet been used in large scale and the regeneration is neither continuous nor on-site.<sup>6–10</sup> An approach to selective adsorbents is molecularly imprinted polymers (MIPs), often referred to as artificial receptors. These are synthetic materials with memory sites, able to selectively recognize and bind specific target molecules. The molecular imprinting technique involves the guided polymerization of a

<sup>a</sup> Leibniz Institute of Surface Engineering e.V. (IOM), Permoserstrasse 15,  
04318 Leipzig, Germany. E-mail: agnes.schulze@iom-leipzig.de

<sup>b</sup> Institute of Chemical Technology, Universität Leipzig, Linnéstraße 3,  
04103 Leipzig, Germany

† Electronic supplementary information (ESI) available. See DOI: <https://doi.org/10.1039/d3qm00345k>


functional monomer and a cross-linker around the template molecule. The subsequent removal of the template molecule results in specific binding sites matching the size, shape, and spatial orientation of the original template molecule.<sup>11</sup> Numerous research studies investigated the adsorption efficiency and selectivity of MIPs *via* different polymerization routes and using various types of functional monomers. Zhongbo *et al.*<sup>12</sup> reported the preparation of MIPs *via* precipitation polymerization with a maximum adsorption capacity of 26.15 mg g<sup>-1</sup> for E2. Furthermore, Lin *et al.*<sup>13</sup> proved that 100 mg of MIP microspheres, prepared with 4-vinylpyridine as the functional monomer and trimethylolpropane trimethacrylate as the cross-linker, had a higher removal selectivity and efficiency than 100 mg or even 300 mg of activated carbons, and a reusability of 30 times. Santos Xavier *et al.*<sup>14</sup> investigated the polarity of the solvent used for polymerization and suggested using acetonitrile as the porogen, which increased the adsorption capacity of MIPs for E2 (37.1 mg g<sup>-1</sup>). The increasing number of research studies on the use of imprinted polymers to remove various micropollutants from water demonstrates the presumed potential of this technique. On the other hand, using small imprinted particles in adsorption processes generally generates too high backpressure and material losses.<sup>15</sup> Molecularly imprinted membranes (MIMs), a new class of membranes containing MIP particles as selective adsorbents, could solve these problems. Several research studies have investigated the use of MIPs to introduce selectivity to membranes and thus increasing the membrane adsorption capacity. MIMs can benefit from both the imprinting technique by introducing extra specific adsorption sites to the membrane and the membrane separation technique (*e.g.*, continuous separation process, low energy consumption, easy scaling up). Niedergall *et al.*<sup>16</sup> investigated the synthesis of adsorbent nanoparticles (NPs) using a mini-emulsion polymerization technique. The NPs were then embedded in a membrane to produce nanostructured adsorber membranes, which were efficiently used to remove bisphenol A (BPA) from water. Gkementzoglou *et al.*<sup>17</sup> used a similar technique, employing sodium dodecyl sulfate (SDS) as a surfactant and atrazine as the target molecule to prepare NPs. These NPs were used to fabricate a sandwich-type membrane consisting of two polyamide support membranes for the selective adsorption of the target atrazine from aqueous systems.

In this study, an approach for synthesizing composite polyethersulfone (CPES) membranes is presented. The method involves the synthesis of MIP particles imprinted with E2 through precipitation polymerization using methacrylic acid as the functional monomer. Three different types of cross-linkers, namely trimethylolpropane trimethacrylate (TRIM), ethylene glycol dimethacrylate (EGDMA), and divinylbenzene (DVB), are utilized to attain the optimal particle properties to be embedded in composite membranes. A control experiment is conducted to prepare non-imprinted polymer particles (NIP) *via* the same procedure in the absence of E2. Batch adsorption experiments are carried out to investigate the affinity and selectivity properties of the particles. Subsequently, composite imprinted membranes,

embedded with either MIP or NIP particles, are prepared *via* a phase inversion process. The optimal particle to polymer solution ratio is investigated for the best adsorption performance. Blank PES membranes without the addition of particles are also prepared and tested as a control. The composite membranes are then irradiated with an electron beam accelerator to fix the polymer particles inside the membrane scaffold. The exposure of the composite membranes to electron beam irradiation leads to the formation of various activated species, including radicals. These radicals have the potential to undergo recombination reactions, resulting in the formation of covalent bonds.<sup>18,19</sup>

Unlike modifications with UV light, which has limited penetration depth, electron beam irradiation can penetrate the entire cross-section of the membrane, resulting in more comprehensive and thorough modifications. Moreover, electron beam irradiation does not require hazardous polymerization initiators or other toxic reagents, making it an environmentally friendly option. Additionally, electron beam irradiation is a directed and fast technique that can produce modifications quickly, making it an attractive option for industrial applications.<sup>20,21</sup> Sandwich-like membranes filled with particles are subjected to batch and dead-end filtration experiments to determine the static and dynamic adsorption loading and selectivity. Adsorption isotherm models are developed, and the best fitting model with the experimental adsorption data is identified. Finally, a simple and effective regeneration procedure is developed, and the composite membranes are reused for ten subsequent cycles, making this approach suitable for sustainable processes.

The composite membranes synthesized in this investigation exhibited significant adsorption capacity for E2, even in the presence of other molecules. Furthermore, the composite membranes were successfully regenerated and reused in ten consecutive cycles, maintaining their original adsorption capacity without any major loss. The composite membranes were also tested with real water samples, exhibiting comparable dynamic adsorption loadings to the experiments with ultrapure water samples.

## Experimental

### Materials and methods

17 $\beta$ -estradiol (E2), citalopram (CIT), methacrylic acid (MAA), divinylbenzene (DVB), trimethylolpropane trimethacrylate (TRIM), ethylene glycol dimethacrylate (EGDMA), bisphenol A (BPA), 2,2'-azobis (2-methylpropionitrile) (AIBN), methanol (MeOH), acetic acid, acetonitrile (ACN) and 1-methyl-2-pyrrolidone (NMP) were purchased from Sigma Aldrich (St. Louis, USA). Polyethersulfone (PES, Ultrason E2010) was purchased from BASF, Ludwigshafen, Germany. Polyethylene glycol 400 (PEG) was purchased from Acros Organics, part of Thermo Fisher Scientific (Geel, Belgium). Toluene, aluminum dioxide and absolute ethanol, were purchased from VWR (Radnor, USA). Fluorescent detection (Infinite M200, Tecan, Germany), microcentrifuge (Carl Roth, Karlsruhe, Germany). Shaker (Vibramax 100, Heidolph, Schwabach, Germany).



Mixer (SpeedMixer DAC 150.1 FVZ-K, Hauschild engineering, Hamm, Germany). The ultra-pure water was produced by a Milli-Q water purification system. Tap water from the city of Leipzig was used for the real water experiments.

### MIP/NIP particles

**Particle polymerization.** The MIP particles were synthesized using precipitation polymerization, following the protocol described by Celiz *et al.*<sup>22</sup> In this work, E2 was selected as the template molecule (1 mmol), methacrylic acid (MAA) was used as the functional monomer (8 mmol), and DVB, EGDMA, or TRIM were employed as cross-linkers (40 mmol). This ratio of 1 : 8 : 40 of the template, functional monomer, and cross-linker has been previously reported to be successful for imprinting various hormones.<sup>23</sup> The pre-polymerization mixture containing the template, functional monomer, and cross-linker was dissolved in a mixture of acetonitrile and toluene (3 : 1, v/v) as a porogen, in a three-neck flask. The mixture was sonicated for 15 min to achieve homogeneity, degassed with gentle nitrogen flow for 20 min, and sealed. The initiator, AIBN (2 wt% of the monomers), was dissolved in a trace amount of acetonitrile and then added to the mixture *via* injection. The flask was attached to a mixer, and the mixture was stirred at approximately 150 rpm in a silicon oil bath at 70 °C for 2 h. The resulting polymer was collected by precipitation using a microcentrifuge (Carl Roth, Karlsruhe, Germany). The template and non-polymerized monomers were removed *via* a washing procedure: 50 mL of a methanol/acetic acid solution (9 : 1, v/v) was added to the polymer, and the mixture was sonicated for 15 min. The mixture was centrifuged at 6000 rpm for 20 min, and the supernatant solution was decanted. This procedure was repeated six to eight times until no template molecules were detected with fluorescence at an excitation wavelength of 276 nm and an emission wavelength of 305 nm in the supernatant solution. The polymers were then washed with absolute ethanol to remove the acetic acid, and the polymer particles were dried overnight at 50 °C. The corresponding non-imprinted polymer (NIP) particles were prepared using the same protocol, without the addition of the template molecule.

### Morphology

In order to examine the morphology of the particles, a suspension solution of MIP or NIP particles in ethanol, amounting to 50 µL, was deposited on a silicon wafer and subsequently allowed to dry at room temperature. The resultant morphology and size of the MIP and NIP particles were assessed using an Ultra 55 Scanning Electron Microscope (SEM) (Carl Zeiss Ltd, Göttingen, Germany) with magnifications ranging from 1000 to 10 000.

### Batch rebinding, imprinting, and selectivity studies

The rebinding properties of the synthesized particles were examined by conducting adsorption experiments on E2 in aqueous solution, using MIP or NIP particles. Specifically, 10 mg of different MIP or NIP particles were added to 15 mL falcon tubes containing an aqueous ethanol/water solution

(1 : 9, v/v) solution of E2 at a concentration of 10 mg L<sup>-1</sup>. The mixture was then vortexed for 10 s and placed on a shaker for a duration of 30 min, allowing the powders to rebinding the target analyte. Subsequently, 1 mL of the resulting solutions was collected and centrifuged at 6000 rpm for 10 min, in order to isolate the solid phase. The concentration of free E2 in the solution was measured through fluorescence detection, and the adsorption loading ( $Q_{\text{ads}}$ , mg g<sup>-1</sup>) of the synthesized particles was measured using eqn (1).

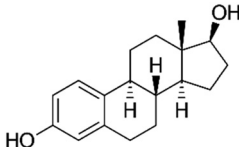
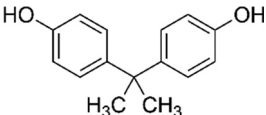
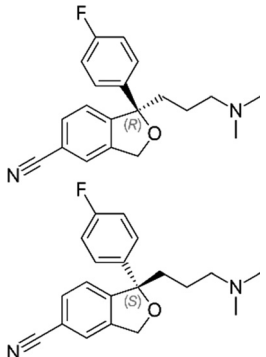
$$Q_{\text{ads}} = (C_0 - C_f) \times \frac{V}{m} \quad (1)$$

where  $C_0$  (mg L<sup>-1</sup>) is the initial concentration of E2 before adsorption,  $C_f$  (mg L<sup>-1</sup>) is the free concentration of E2 remaining in the solution after adsorption process,  $V$  (L) corresponds to the volume of the solution and  $m$  (g) signifies the mass of the used particles.

The imprinting factor (IF) of the particles was calculated using eqn (2), comparing the adsorption loading of MIP and NIP particles towards E2.

To evaluate the selectivity factor (SF) of the MIP particles, 10 mg of MIP particles were dispersed in 15 mL solutions of E2 or BPA solution with an initial concentration of 10 mg L<sup>-1</sup>. Following a 30 min incubation period, the changes in the respective concentration levels were quantified through fluorescence detection. The excitation wavelength and emission wavelength for BPA were 270 nm and 310 nm, respectively. Table 1 presents a summary of the molecules examined along with their respective properties.

**Table 1** Investigated molecules and their properties

Compound	Chemical structure	Molecular weight/g mol <sup>-1</sup>	log $K_{\text{ow}}$
17β-Estradiol (E2)		272.4	4.01 <sup>24</sup>
Bisphenol-A (BPA)		228.3	3.32 <sup>24</sup>
Citalopram (CIT)		324.4	1.39 <sup>25</sup>





SF was calculated utilizing eqn (3), which entails comparing the adsorption loading of MIP particles towards E2 with their adsorption loading towards BPA.

$$IF = \frac{Q_{\text{ads-MIP}}}{Q_{\text{ads-NIP}}} \quad (2)$$

$$SF = \frac{Q_{\text{ads-MIP}}^{\text{E2}}}{Q_{\text{ads-MIP}}^{\text{BPA}}} \quad (3)$$

### Composite membranes

**Fabrication of composite membranes.** Flat sheet polyether-sulfone (PES) membranes were fabricated *via* a non-solvent induced phase inversion process.<sup>26</sup> The membrane composition consisted of 14 wt% PES, 21 wt% NMP as the solvent, and 65 wt% PEG as the pore-forming agent. Composite membranes were prepared by adding the synthesized MIP or NIP particles to the polymer solution in a specific ratio, followed by mixing for 30 min at 3500 rpm using a mixer (SpeedMixer DAC 150.1 FVZ-K, Hauschild engineering, Hamm, Germany) until a homogeneous mixture was obtained. The content of MIP and NIP particles ranged between 0 and 4 wt% of the polymer solution. The resulting viscous membrane dope solution was spread onto a glass plate using a casting knife with a gap width of 200  $\mu\text{m}$  and a custom-made automated casting system. Subsequently, the polymer film was transferred to a water vapor chamber at room temperature for 5 min and then immersed in a water tank containing cooled ultrapure water ( $\sim 10^\circ\text{C}$ ) for 5 min. Finally, the membranes were thoroughly rinsed with ultrapure water. During the membrane formation process, the MIP and NIP particles, which are insoluble in water and NMP, were embedded in the PES membrane matrices to form composite membranes. To ensure covalent immobilization of the particles in the membrane scaffold, the composite membranes were irradiated in the wet state with an irradiation dose of 150 kGy under a  $\text{N}_2$  atmosphere with  $\text{O}_2$  quantities lower than 10 ppm using a self-built electron accelerator. The voltage was set to 160 kV, while the current was adjusted to 10 mA. The irradiation dose was regulated by controlling the speed of the sample transporter. The membranes were then air-dried at room temperature. To prepare the reference PES membrane, a membrane was fabricated using the same procedure as mentioned above but without the addition of the MIP or NIP particles.

### Membranes characterization

To fully characterize the membranes, various measurements were conducted including SEM, XPS, water permeance, water contact angle, and Hg porosimetry. The Ultra 55 SEM (Carl Zeiss Ltd, Göttingen, Germany) was used to investigate the surface morphology and the cross-sectional area of the reference and composite membranes under magnifications ranging from 1000 to 25 000. The membrane samples were manually cut and coated with a thin (30 nm) chromium film using the Z400 sputter system (Leybold, Hanau, Germany). XPS (Kratos

Axis Ultra, Kratos Analytical Ltd, Manchester, UK), was employed to analyse the chemical composition of the top surface of the reference and composite membranes.

Pore size distribution and bulk porosity of the membranes were determined with the mercury porosimeter PoreMaster 30 (Quantachrome Instruments, Odelzhausen, Germany). The water contact angle was determined using the sessile drop method with a static water contact angle measurements system (DSA 30E, Krüss, Hamburg, Germany). Values of at least three different samples were averaged.

The permeation studies were performed using a stainless-steel filtration cell (16 249, Sartorius Stedim Biotech, Göttingen, Germany). The time taken to filter 50 mL of deionized water at a pressure of 1 bar was recorded. The average permeation time was calculated for three individual samples. Water permeance  $J$  ( $\text{L h}^{-1} \text{m}^{-2} \text{bar}^{-1}$ ) was calculated *via* eqn (4).

$$J = \frac{V}{t \cdot A \cdot P} \quad (4)$$

where  $V$  (L) denotes the volume of water passed through the membranes,  $t$  (h) addresses the permeation time,  $A$  ( $\text{m}^2$ ) is the upper surface area of the membrane, and  $P$  (bar) is the applied pressure. The bubble point of wet membranes was checked by continuously increasing the pressure to a point at which the first stream of bubbles emerges.

### Static adsorption tests

The present study conducted static adsorption experiments using a procedure previously described in our work.<sup>27</sup> To summarize, a concentrated stock solution of E2 in absolute ethanol with a concentration of  $10 \text{ mg mL}^{-1}$  was prepared, which was subsequently diluted with an ethanol/water solution (1:9, v/v) to obtain a diluted estradiol stock solution with a concentration of  $5 \text{ mg L}^{-1}$ . Subsequently, 200  $\mu\text{L}$  of  $5 \text{ mg L}^{-1}$  E2 solutions were added to 10 mm membrane disks placed in a 48-well microtiter plate, and shaken for 30 min.

The supernatant solution was then collected and transferred to a new microtiter plate. Finally, the concentration of E2 was determined by fluorescence detection, and the adsorbed amount of E2 (%) was calculated using eqn (5):

$$\text{E2 adsorbed (\%)} = \frac{C_0 - C_f}{C_0} \times 100 \quad (5)$$

where  $C_0$  ( $\text{mg L}^{-1}$ ) is the initial concentration of E2 before adsorption,  $C_f$  ( $\text{mg L}^{-1}$ ) is the free concentration of E2 remaining in the solution after adsorption process.

### Dynamic adsorption loading

Dynamic adsorption loadings of the composite and reference membranes were investigated using a dead-end filtration setup. Aqueous solutions of micropollutants with known initial concentrations  $C_0$  were prepared according to the procedure outlined in the previous section. The aqueous solution of each micropollutant was passed through the membranes (active area  $17.4 \text{ cm}^2$ ) using a stainless-steel pressure filter holder (16 249, Sartorius, Germany). The filtration process began with the



wetting of the membrane with 20 mL of water/ethanol solution (9:1, v/v). Different volumes of the aqueous E2 solution were first poured in the filtration cell and then forced through the composite membranes under a constant N<sub>2</sub> pressure of 16 mbar. 500 µL of permeate was collected at every 10 mL intervals to quantify the concentration of the E2 in the permeate (C<sub>p</sub>).

The dynamic adsorption loading Q<sub>dyn</sub> (mg g<sup>-1</sup>) was calculated at the breakthrough (BT) point, (defined at a C<sub>p</sub> of 10% relative to C<sub>0</sub>) according to eqn (6):

$$Q_{\text{dyn}} = \frac{m_{\text{ads}}}{m_{\text{membrane}}} \quad (6)$$

For which the amount adsorbed m<sub>ads</sub> was determined by numerical integration of the BT curve data points between V<sub>0</sub> and V<sub>BT</sub> with OriginPro 2019b (OriginLab) and m<sub>membrane</sub> (g) denotes the weight of the membrane used.

### Stability

To demonstrate the stability of the composite and the reference PES membranes and the success of fixing the particles in the membrane scaffold, continuous Soxhlet extraction for 7 d in boiling water was performed. The amount of total organic carbon (TOC) extracted from the membranes into the water was investigated using the TOC analyzer system liquiTOC II (Elementar Analysensysteme GmbH, Hanau, Germany).

### Selectivity and binding affinity

To further demonstrate the binding affinity and selectivity of the composite membranes, imprinting factor (IF) and selectivity factor (SF) were calculated.

The IF demonstrates the affinity of the CPES membranes with the imprinted particles towards E2 compared to CPES membranes with non-imprinted particles or the reference PES membrane and is calculated *via* eqn (7).

$$\text{IF} = \frac{Q_{\text{dyn}}^{\text{MIP-CPES-EB}}}{Q_{\text{dyn}}^{\text{x}}} \quad (7)$$

where Q<sub>dyn</sub><sup>MIP-CPES-EB</sup> is the dynamic adsorption loading of the irradiated CPES membrane with MIP particles, and x denotes either adsorption loading of the irradiated CPES membrane with NIP particles or reference PES membrane.

Selectivity of the MIP-CPES membranes were investigated performing dynamic adsorption tests using solutions containing E2, BPA, and CIT individually or in a mixture.

The excitation and emission wavelength for CIT are 249 nm and 302 nm, respectively. The initial concentration of each of the molecules was 5 mg L<sup>-1</sup> (a total of 15 mg L<sup>-1</sup> in the mixture solution). The selectivity factor was calculated using eqn (8).

$$\text{SF} = \frac{Q_{\text{E2}}^{\text{MIP-CPES-EB}}}{Q_{\text{x}}^{\text{MIP-CPES-EB}}} \quad (8)$$

where Q<sub>E2</sub><sup>MIP-CPES-EB</sup> is the dynamic adsorption loading of MIP-CPES membrane towards E2 and Q<sub>x</sub><sup>MIP-CPES-EB</sup> is the dynamic adsorption loading of MIP-CPES towards BPA or CIT.

### Adsorption isotherms

Adsorption isotherms were investigated *via* dynamic adsorption tests at various template concentrations in the solute, adapting the procedure reported by Semiao *et al.*,<sup>28</sup> where different volumes of E2 solutions with a concentration in the range of 2–10 mg L<sup>-1</sup> were passed through the membrane. The experimental data were fitted with a linearized form of the Langmuir equation (eqn (9)).

$$\frac{C_e}{Q_{\text{dyn}}} = \frac{C_e}{q_m} + \frac{1}{q_m \times K_L} \quad (9)$$

where C<sub>e</sub> (mg L<sup>-1</sup>) is the free concentration of E2 in the filtered solution after the membrane has reached saturation and no more adsorption is taking place. In eqn (9), q<sub>m</sub> (mg g<sup>-1</sup>) is the maximum monolayer loading of the adsorbate on the membrane and K<sub>L</sub> (L g<sup>-1</sup>) is the Langmuir constant which denotes the adsorption affinity of the solute on the adsorbent.

The data were also fitted with a linearized form of the empirical Freundlich equation (eqn (10)).

$$\log Q_{\text{dyn}} = n \times \log C_e + \log K_F \quad (10)$$

where K<sub>F</sub> ((mg m<sup>-2</sup>) (mg L<sup>-1</sup>)<sup>-n</sup>) is the Freundlich constant which denotes the adsorption affinity, while *n* is the Freundlich exponent (dimensionless).

### Regeneration

To test the reusability of the synthesized composite membranes, membranes were washed with water/ethanol solution. After every dynamic adsorption test, 25 mL of water/ethanol solution (1:1, v/v) was passed through the membrane at a pressure of 30 mbar. Followed by another filtration with a diluted water/ethanol solution (9:1, v/v). Afterwards, the regenerated membranes were applied to another cycle of dynamic adsorption. This procedure was repeated for each dynamic adsorption test for five to ten times. The adsorption capacities of the regenerated membranes were compared with the not regenerated ones.

## Results and discussion

### MIP/NIP particles

Different methods have been explored and published in the literature for the synthesis of molecularly imprinted polymer (MIP) particles. Precipitation polymerization is straightforward and uncomplicated method that involves the mixing of template, monomers, initiator, and porogen in a single step. To prevent the formation of monolithic structures, a low monomer amount is commonly employed.<sup>29</sup> In this study, different cross-linkers were examined to fabricate microspheres that are suitable for integration into membranes for separation applications. Acetonitrile/toluene (3:1) was employed as porogen to minimize hydrogen bonding interference while increasing microsphere porosity.<sup>30</sup> The synthesized polymer particles were washed, and the template was extracted with a solvent that could disrupt the interactions between the template and the



polymer scaffold (methanol/acetic acid, 9:1, v/v). This step generates adsorption sites that are capable of re-binding the template.<sup>31</sup> The composition of the synthesized particles is provided in Table S1 (ESI<sup>†</sup>).

### Particle morphology

Fig. 1 illustrates morphology of MIP and NIP particles fabricated with DVB as a cross-linker in the polymerization. The polymerization yielded particles with an almost perfect spherical shape, measuring  $2 \pm 1 \mu\text{m}$  in size. The spherical properties of the synthesized particles were deemed satisfactory for their potential use as adsorbent particles in the membrane scaffold. The SEM images of the particles synthesized with TRIM and EGDMA are provided in Fig. S1 (ESI<sup>†</sup>).

### Particle adsorption loading

The ability of the MIP particles to selectively (re)adsorb E2 over the NIP particles was assessed by analyzing their adsorption loading and specificity. The binding interactions between E2 and the MIP particles were investigated to determine if they were due to specific interactions with the imprinted selective sites or non-specific interactions with the polymeric backbone found in both MIP and NIP particles.

Batch adsorption tests were performed to evaluate the adsorption performance of the synthesized imprinted and non-imprinted particles. The concentration of E2 after 30 minutes was measured using fluorescent detection (Infinite M200, Tecan, Germany). Fig. 2 depicts the adsorption capacities of MIP and NIP particles prepared with DVB as cross-linker.

The MIP particles exhibit higher E2 adsorption loading compared to their corresponding NIPs due to the imprinting process during particle synthesis. During polymerization, functional monomers assembled around the E2 molecules in an ordered manner *via* hydrogen bonds, and their positions were fixed by the cross-linker. Upon extraction of the template, a molecular memory site was created in the polymer matrix, creating cavities that were complementary to E2 molecules, enabling the particles to recognize and rebind the template. Conversely, the random distribution of functional monomers in the NIP particles resulted in a lower binding affinity for E2. The E2 adsorption loading for MIP is  $13.9 \pm 1.3 \text{ mg g}^{-1}$ ,

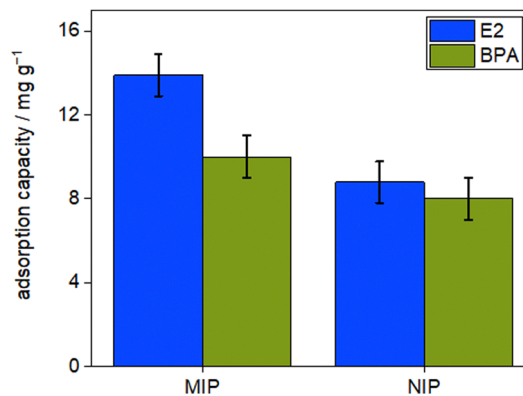


Fig. 2 Adsorption capacity of MIP and NIP particles prepared with DVB as cross-linker towards E2 and BPA.

whereas the corresponding NIP exhibited an adsorption loading of  $8.8 \pm 0.8 \text{ mg g}^{-1}$ . The imprinting factor (IF), a metric for determining the success of the imprinting process, was calculated to compare the adsorption capacities of MIP and NIP particles towards E2 using eqn (2). MIP and NIP particles prepared with DVB as the cross-linker demonstrated the highest IF, with a value of 1.6.

In order to investigate the specificity of the synthesized particles, the adsorption loading of MIP and NIP particles were evaluated in a different solution containing BPA with the same initial concentration of  $10 \text{ mg L}^{-1}$ . As anticipated, the adsorbed amount of E2 for the MIP particles was greater than the adsorbed amount of BPA. The selectivity factor (SF) for the imprinted particles was calculated using eqn (3). MIP particles showed a high SF with a value of 1.4, indicating that adsorption is governed by specific binding of E2 to the imprinted sites. These findings are consistent with the work of Celiz *et al.*,<sup>22</sup> who employed molecularly imprinted polymer for the isolation/enrichment of 17 $\beta$ -estradiol. In the literature, it has been reported that the adsorption capacity obtained by Jiang *et al.*<sup>10</sup> using graphene oxide nanosheets as E2 adsorbent was approximately  $149 \text{ mg g}^{-1}$  in 12 hours. Fukuhara *et al.*<sup>32</sup> obtained a value of 21.3 to  $67.6 \text{ mg g}^{-1}$  using eight different types of activated carbon. Despite our values being lower than those reported in the literature for activated carbon, the advantage of our polymers lies in their selectivity and ease of regeneration, which are not present in the traditional adsorbents. MIP particles prepared with DVB as cross-linker exhibited high IF and SF values and were chosen to be employed as the adsorbent particles in the membrane scaffold. The adsorption capacities of MIP and NIP particles prepared with EGDMA and TRIM and their corresponding IF and SF values are presented in Fig. S2 and Table S2 (ESI<sup>†</sup>), respectively.

### Composite membranes

In order to fabricate composite membranes incorporating MIP or NIP particles, the phase inversion technique was utilized. During the membrane formation process, the casting solution, containing MIP or NIP particles, was inverted to a solid porous membrane in a non-solvent (water). Since MIP and NIP

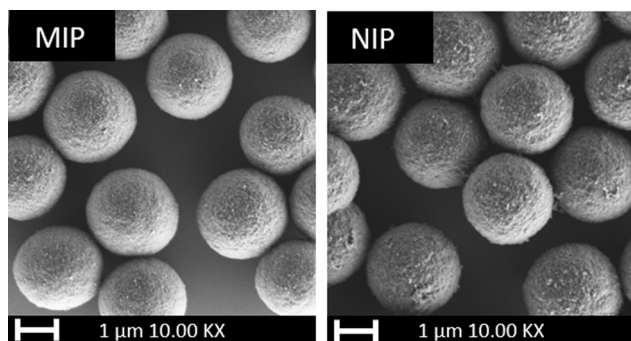


Fig. 1 SEM images of MIP and NIP particles prepared with DVB as cross-linker.





particles are insoluble in water or NMP, the resulting PES membrane contained the unchanged MIP or NIP particles embedded within it, without significant alteration of the PES membrane structure.

### Particle loading quantity

In order to determine the optimal particle to polymer solution ratio for adsorption performance, the loading content of the MIP particles was varied from 0 wt% (*i.e.*, the reference non-particle loaded PES) to 4 wt% of the dope solution. Static adsorption tests were subsequently conducted, and the adsorbed E2 (%) was determined using eqn (5). The adsorbed amount of E2 (%) as a function of the synthesized membranes containing various quantities of MIP particles is presented in Fig. 3. The results indicate that the PES membrane without MIP particles exhibited the lowest binding capacity, removing only 40% of the E2 initially present in the solution. As the loading content of the MIP particles increased, the binding capacity of the composite membranes also increased. Notably, membranes containing 4 wt% MIP particles demonstrated exceptional adsorption performance, removing over 95% of the initial E2 from solution. Based on these results, the 4 wt% particles to polymer solution ratio was deemed optimal and was further investigated. It is important to emphasize that increasing the loading quantity is not without limitation, as excessive loading may have adverse effects on the strength and structure of the PES membranes.<sup>33</sup>

### Membrane performance

The composite membranes that were irradiated, as well as the reference PES membrane, underwent a comprehensive characterization through various techniques. The surface morphology and cross-sectional structure of the membranes were observed using SEM. Water permeance measurements were conducted to assess the alterations in membrane performance with respect to flux. Mercury porosimetry was implemented to detect any possible pore narrowing in the membrane's pores. Water contact angle analysis was performed to investigate changes in

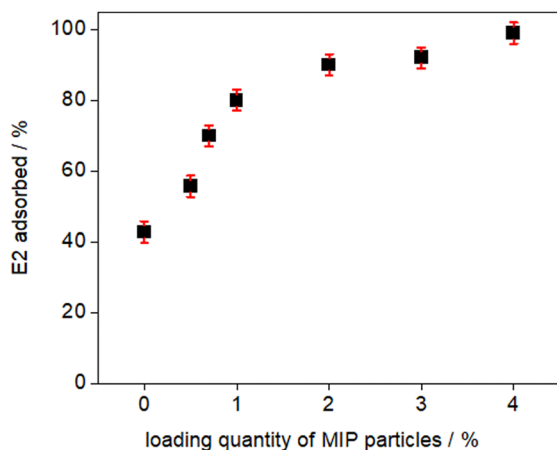


Fig. 3 E2 adsorption (%) as a function of MIP loading quantity in the membrane scaffold.

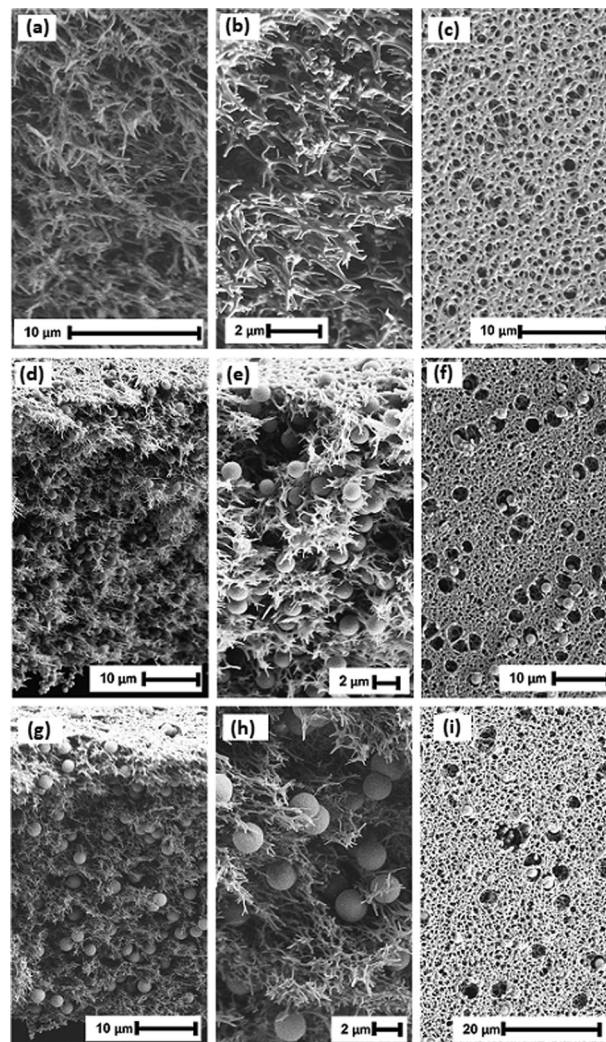


Fig. 4 SEM images of the (a) and (b) cross-section and (c) top side of the reference PES membrane, and (d) and (e) cross-section and (f) top side of MIP-CPES-EB membrane, and (g) and (h) cross-section and (i) top side of the NIP-CPES-EB membrane.

membrane hydrophilicity, and XPS analysis was conducted to determine the chemical composition of the membrane surface. The SEM images presented in Fig. 4a, b and c exhibit a symmetric open pore structure for the reference PES membrane. The particle-loaded membranes on the other hand, demonstrated a uniform distribution of the particles both in cross-section and on the surface of the membranes. The membrane formation process successfully deposited polymer particles in the membrane structure's pores, and these particles were freely accessible without forming any macro voids. The SEM images confirmed that there was no agglomeration of particles in the membrane scaffold. Both MIP-CPES-EB and NIP-CPES-EB membranes exhibited some cavity structures on their surfaces, which could be attributed to the particles escaping into the water phase during the phase-inversion process.

The reference PES membrane demonstrated a permeance of  $16\,468 \pm 1600 \text{ L h}^{-1} \text{ m}^{-2} \text{ bar}^{-1}$ , which slightly decreased for the





composite membranes due to the presence of particles blocking some pores. The porosity and average pore size of the reference PES membrane was identified to be 64% and 0.39  $\mu\text{m}$ , respectively. The porosity of the composite membranes increased to around 70%, and the average pore size decreased from 0.39  $\mu\text{m}$  to 0.21  $\mu\text{m}$  and 0.17  $\mu\text{m}$  for MIP-CPES-EB and NIP-CPES-EB, respectively. These changes can be attributed to the presence of the porous particles in the membranes scaffold. The WCA analysis revealed that the PES reference membrane had a hydrophilic surface with a WCA of  $44^\circ$ , whereas the composite membrane exhibited slightly increases surface wettability, with contact angle values of  $39^\circ$  and  $37^\circ$  for MIP-CPES-EB and NIP-CPES-EB, respectively. The presence of cavities on the composite membrane surface contributed to this increase in hydrophilicity, as the surface roughness and structure also played a role in the WCA. XPS analysis confirmed that embedding the particles in the membranes did not alter the chemical compositions of the top surface of the membranes. The results demonstrated that all the membranes had a composition of approximately 75% C, 18% O, and 6% S. Table 2 summarizes all the characterizations conducted.

### Stability

To investigate the stability of the composite membranes and the immobilized particles inside the membrane scaffold, the membrane samples were exposed to a continuous Soxhlet extraction for 7 d in boiling water. Extracted material including non-immobilized MIP or NIP particles, or degraded membrane polymer, were detected by measuring the total organic carbon (TOC) of the extraction water. Fig. 5 presents the results of the TOC measurements. The results indicate that the reference PES membrane is relatively stable, with a detected TOC amount of  $0.35 \pm 0.05 \text{ mg L}^{-1} \text{ cm}^{-2}$ . On the other hand, the composite non-irradiated membranes had higher TOC values compared to the reference PES membrane. However, electron beam irradiation of the composite membranes led to a significant decrease in the extracted TOC values. This suggests that the MIP and NIP particles are well-fixed in the membrane matrices, potentially due to a cross-linking mechanism. Similar mechanism have been described previously in the literature.<sup>34</sup>

### Breakthrough curves

The present study applies the technique of electron-beam induced grafting to immobilize particles within a membrane scaffold. The grafting process involves immersing composite membranes in ultrapure water, followed by electron beam irradiation. Dynamic adsorption experiments were conducted

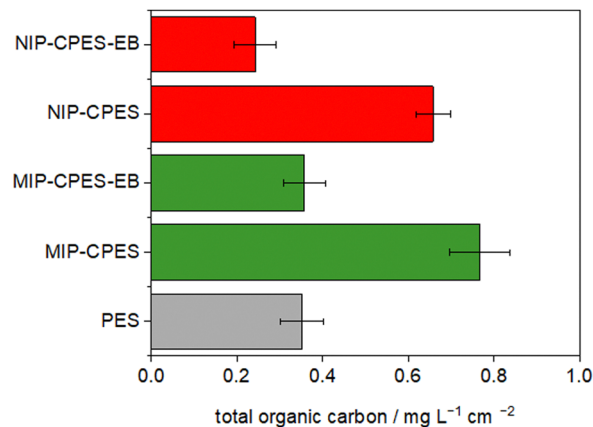


Fig. 5 Total organic carbon in extracted water after 7 d of Soxhlet extraction.

to determine the breakthrough (BT) points of the membranes. The BT point is defined as the point at which the permeate concentration ( $C_p$ ) is 10% of the feed concentration ( $C_0$ ) in a filtration process with a membrane. Dynamic adsorption experiments were performed at a constant pressure of 16 mbar to determine the BT point for E2. 400 mL of aqueous E2 solution with a  $C_0$  of  $5 \text{ mg L}^{-1}$  was passed through the irradiated composite and the reference membrane. 500  $\mu\text{L}$  permeate samples were collected at 20 mL intervals. The concentration of each sample was determined *via* fluorescent detection, with a limit of detection of  $0.1 \text{ mg L}^{-1}$  for E2. Fig. 6 depicts the BT curves for E2 for the composite and reference PES membranes. The concentration of first permeate sample for the reference PES membrane is  $4.7 \text{ mg L}^{-1}$ , indicating that the membrane is already saturated and does not adsorb E2 anymore. The permeate concentration is maintained at nearly constant levels until the entire feed solution is filtered. In contrast, the first permeate sample for the irradiated composite membrane (MIP-CPES-EB) is  $0.1 \text{ mg L}^{-1}$ . This  $C_p$  of  $0.1 \text{ mg L}^{-1}$  remains almost constant until a feed volume of 140 mL is filtered. At this point a steady increase in the permeate concentration is observed. The plateau in the adsorption was reached after filtering 320 mL of the feed solution. Since the reference PES membrane was already saturated at 20 mL, the adsorption of the E2 in case of MIP-CPES-EB is clearly attributed to the adsorptive effects of the imprinted particles and the successful grafting of the imprinted particles onto the membrane scaffold *via* electron beam irradiation. The BT curve for the irradiated composite membranes with non-imprinted particles (NIP-CPES-EB) is illustrated in Fig. 6. The adsorption behaviour of

Table 2 Water contact angle, permeance, average pore size, porosity, and chemical composition of the reference and composite PES membranes

Membrane	WCA/ $^\circ$	Permeance/ $\text{L h}^{-1} \text{ m}^{-2} \text{ bar}^{-1}$	Average pore size/ $\mu\text{m}$	Porosity/%	Chemical composition/relative atom (%)		
					C	O	S
PES	$44 \pm 3$	$16\,468 \pm 1600$	0.39	$64 \pm 2$	75.78	18.74	5.47
MIP-CPES-EB	$39 \pm 2$	$13\,723 \pm 1300$	0.21	$70 \pm 2$	75.51	18.58	5.91
NIP-CPES-EB	$37 \pm 2$	$15\,439 \pm 1500$	0.17	$69 \pm 2$	75.32	18.52	6.16



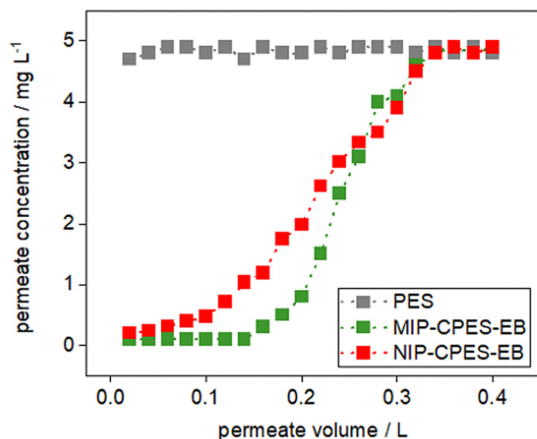


Fig. 6 BT curves for the reference and irradiated composite membranes with imprinted and non-imprinted particles.

the NIP-CPES-EB membrane differs from that of the MIP-CPES-EB membrane. A steady increase in the permeate concentration is observed for irradiated membranes with non-imprinted particles, and the initial permeate concentration was found to be  $0.2 \text{ mg L}^{-1}$ . The NIP-CPES-EB filtered 120 mL of the feed solution until the BT point was reached. The breakthrough curves clearly show that the membranes with imprinted particles have a higher adsorption loading for the target molecule compared to the membranes with the non-imprinted particles. The breakthrough curves for the non-irradiated membranes are shown in Fig. S3 (ESI†).

The dynamic adsorption loading ( $Q_{\text{dyn}}$ ) was determined at the BT point achieved from the breakthrough curves. Fig. 7 presents the dynamic adsorption loadings of the reference and composite membranes. The reference PES membrane exhibited a  $Q_{\text{dyn}}$  of  $1.4 \pm 0.5 \text{ mg g}^{-1}$ . As anticipated from the breakthrough curves, the MIP-CPE-EB exhibited the highest adsorption loading for E2 with a value of  $12.9 \pm 1 \text{ mg g}^{-1}$ . Meanwhile,  $Q_{\text{dyn}}$  was predictably lower for the composite membranes with the non-imprinted particles. NIP-CPES-EB displayed a  $Q_{\text{dyn}}$  of  $7.6 \pm 1 \text{ mg g}^{-1}$ . The dynamic adsorption loading for the non-irradiated membranes are reported in Fig. S4 (ESI†). The results clearly demonstrate that irradiating the membranes improves

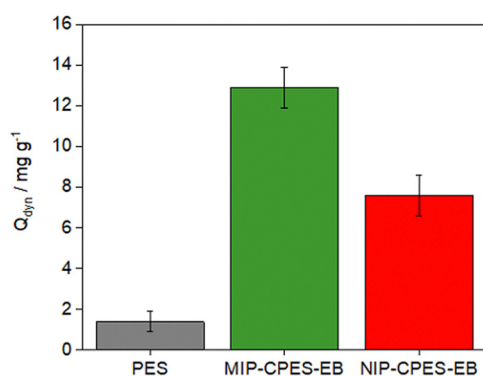


Fig. 7 Dynamic adsorption loadings of the reference and composite membranes measured at the breakthrough point.

the immobilization of the particles inside the membrane scaffold and is a crucial factor in the synthesis of the composite membranes. In a study by Koc *et al.*,<sup>35</sup> the selective removal of E2 using molecularly imprinted particle-embedded cryogel systems resulted in an adsorption loading of  $5.32 \text{ mg g}^{-1}$ . The high adsorption loading of the composite membranes synthesized in our study suggests that employing composite membranes is a more effective approach for removing E2 from water. McCallum *et al.*<sup>36</sup> investigated the adsorption capacity of nanofiltration membranes towards E2 and reported a maximum value of  $0.18 \mu\text{g cm}^{-2}$ . By normalizing the adsorption loading of our NIP-CPES-EB and MIP-CPES-EB membranes to the surface area of the membranes, we obtained values of  $36.4 \pm 1 \mu\text{g cm}^{-2}$  and  $42.3 \pm 1 \mu\text{g cm}^{-2}$ , respectively. The higher adsorption loading of our composite membranes is accompanied by the lower pressure required for filtration and higher water permeation, making these composite membranes a more advantageous option for water purification.

### Selectivity and binding

During the imprinting process, the recognition sites in the imprinted polymer are the primary factors responsible for its template recognition ability. Thus, it is crucial to investigate the presence of specific recognition sites in the membranes containing the imprinted particles. To this end, three separate aqueous solutions, each containing E2, BPA, and CIT at a similar initial concentration of  $5 \text{ mg L}^{-1}$  were prepared.

A volume of 150 mL of each solution was filtered through the composite and the reference PES membranes, and the adsorption loadings were determined at the breakthrough points. The findings are depicted in Fig. 8. The results indicate that the quantity of E2 adsorbed is significantly greater than the other molecules on both composite membranes. The  $Q_{\text{dyn}}$  of MIP-CPES-EB was established as  $12.9 \pm 1 \text{ mg g}^{-1}$  for E2,  $2.7 \pm 0.5 \text{ mg g}^{-1}$  for BPA, and  $0.9 \pm 0.2 \text{ mg g}^{-1}$  for CIT. In order to assess the selectivity of the membrane with the imprinted particles, the SF was computed using eqn (3). The SF of MIP-CPES-EB for E2 over BPA was determined to be 4.7 (14.3 for E2 over CIT). An SF value greater than 1.0 signifies that the membrane removes one molecule with greater affinity

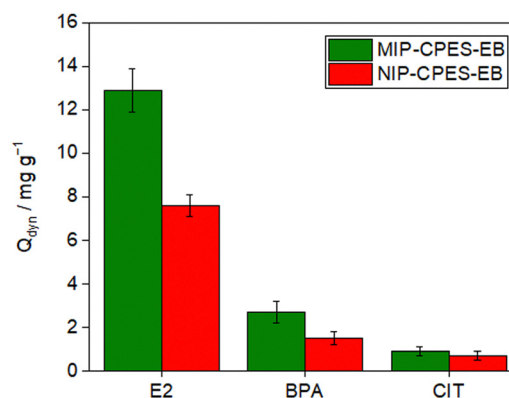


Fig. 8 Adsorption loadings of composite membranes for different hormones.



compared to the other. The high SF values for E2 over BPA and CIT indicate that the membrane is more selective towards E2, relative to the other molecules, thereby affirming the presence of specific recognition sites in the membranes with the imprinted particles.

As discerned from the adsorption loading outcomes depicted in Fig. 7, NIP-CPES-EB, the composite membrane containing non-imprinted particles, exhibited a lower adsorption loading of E2 in comparison to MIP-CPES-EB with a value of  $7.6 \pm 1 \text{ mg g}^{-1}$ . The adsorption loading for BPA and CIT was measured to be  $1.8 \pm 0.5 \text{ mg g}^{-1}$ , and  $0.5 \pm 0.2 \text{ mg g}^{-1}$ , respectively. NIP-CPES-EB relied on the formation of nonspecific interactions between the functional groups present in its structure and those present on the template to bind E2. In contrast, MIP-CPES-EB (fabricated with embedded particles synthesized in the presence of E2) interacted with the template through specific interactions (such as hydrogen bonds<sup>37</sup>) between the functional groups of the template and the complementary recognition sites present in the polymeric particle matrix.

Upon comparison of the adsorption loadings of MIP-CPES-EB and NIP-CPES-EB towards E2, an IF of 1.7 was determined using eqn (2). An IF value exceeding 1.0 indicates that the membrane with the imprinted particles has higher affinity towards the template than the membrane with the non-imprinted particles. Therefore, given the high IF and SF values, it can be affirmed that MIP-CPES-EB contains effective recognition sites with high selectivity and affinity towards E2. Niedergall *et al.*<sup>38</sup> conducted an investigation into efficiency of nanocomposite membrane adsorbents for the removal of micropollutants from water. The adsorbents comprised of nano-scaled spheric polymer adsorbents embedded in PES matrices, which were used to form the nanocomposite membranes. The study reported a maximum adsorption loading of  $7.5 \text{ mg m}^{-2}$  of BPA for imprinted membranes. Normalizing the results to the active surface area, our imprinted membranes (MIP-CPES-EB) exhibited an adsorption loading of  $86.3 \text{ mg m}^{-2}$ , while the non-imprinted membrane (NIP-CPES-EB) exhibited an adsorption loading of  $54.8 \text{ mg m}^{-2}$ . These results suggest that the new approach is highly effective for removing BPA from water due to the high adsorption loading of the composite membranes.

Son *et al.*<sup>33</sup> investigated two effective methods for synthesizing MIP particles. The resulting MIP particles were then used to prepare hybrid membranes that are capable of recognizing and separating BPA and its derivatives from water. Results from the study showed adsorption loadings ranging from  $4.9 \text{ mg g}^{-1}$  to  $10.4 \text{ mg g}^{-1}$  at a particle loading of 4 wt%, which is consistent with our own findings.

The adsorption loadings of both composite membranes were evaluated in a mixed solution containing E2, BPA, and CIT (Fig. 9). The SF values were calculated using eqn (3), which revealed that the composite membrane with imprinted particles can preferentially adsorb E2 over BPA or CIT in a mixture (SF: 6.25 for E2 over BPA and SF: 12.5 for E2 over CIT). This higher molecular recognition of MIP-CPES-EB to its template molecules indicates the successful creation of imprinted

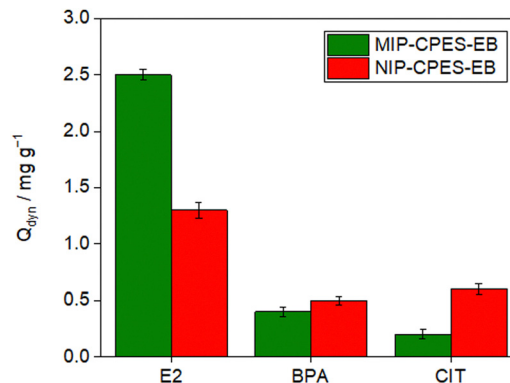


Fig. 9 Adsorption performance of composite membranes in a mixture of E2, BPA and CIT.

cavities during the polymerization process based on the interaction of size, shape, and functionality to the template molecules. The adsorption loading of MIP-CPES-EB in the mixture solution was  $2.4 \pm 0.2 \text{ mg g}^{-1}$  for E2,  $0.4 \pm 0.1 \text{ mg g}^{-1}$  for BPA, and  $0.3 \pm 0.1 \text{ mg g}^{-1}$  for CIT.

### Adsorption isotherms

To further study the binding capacity of the MIP-CPES-EB and NIP-CPES-EB for E2, the adsorption isotherms were investigated. Fig. 10 depicts the Freundlich and Langmuir isotherm plots for both membranes as a function of E2 concentration varying from 2 to  $10 \text{ mg L}^{-1}$ . The adsorption loading of E2 on both membranes increased with the increase in the initial concentration. The data acquired for both membranes was well-fitted to the Langmuir model, implying that monolayer recognition sites were uniformly distributed on the membrane's surface and that E2 was adsorbed through monolayer adsorption onto the adsorption sites. Table 3 shows the corresponding isotherm parameters normalized to the weight of the membranes. The maximum monolayer adsorption loading ( $q_m$ ) increased from  $14.7 \text{ mg g}^{-1}$  on NIP-CPES-EB to  $21.9 \text{ mg g}^{-1}$  on MIP-CPES-EB, indicating a higher binding site density on the composite membrane with imprinted particles. The adsorption affinities expressed by  $K_F$  and  $K_L$ , also confirm significant improvement in the adsorption of E2 on MIP-CPES-EB. The results demonstrate that MIP-CPES-EB is capable of recognizing and adsorbing a larger amount of E2 than NIP-CPES-EB.

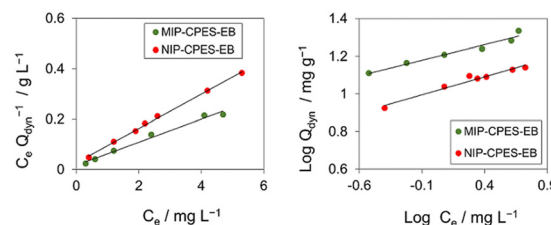


Fig. 10 Experimental data fitted with Langmuir (left) and Freundlich (right) isotherms regarding the adsorption of E2 on composite PES membranes loaded with imprinted or non-imprinted particles (MIP-CPES-EB and NIP-CPES-EB, respectively).





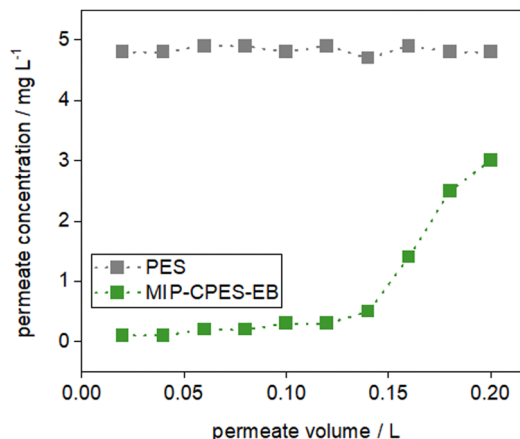
**Table 3** Parameters of the Freundlich and Langmuir isotherm for adsorption of E2 on composite membranes

Membrane	Freundlich			Langmuir		
	$K_F/(\text{mg g}^{-1})$ $(\text{mg L}^{-1})^{-n}$	$n$	$R^2$	$q_m/\text{mg g}^{-1}$	$K_L/\text{L mg}^{-1}$	$R^2$
NIP-CPES-EB	10.4	0.19	0.96	14.7	2.5	0.99
MIP-CPES-EB	15.7	0.16	0.95	21.9	2.8	0.98

### Application in real water samples and regeneration

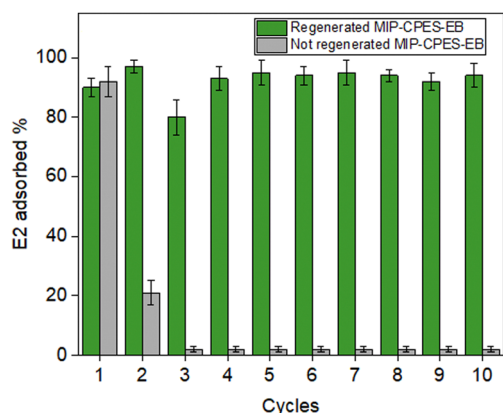
To investigate the regeneration ability, adsorption capacities were analysed over ten binding/regeneration cycles. The regeneration procedure was conducted as follows: 200 mL of aqueous E2 solution with a  $C_0$  of  $5 \text{ mg L}^{-1}$  was passed through each membrane using a filtration cell at a constant pressure of 16 mbar. The permeate was collected and its concentration was measured using fluorescent detection. The adsorption capacity was calculated using eqn (5). After each filtration cycle, the membrane was regenerated using the following steps: first, it was filtered with 25 mL of a water/ethanol (1:1, v:v) solution, followed by another 25 mL of a diluted water/ethanol (9:1, v:v) solution. The regenerated membrane was then subjected to another adsorption cycle. This procedure was repeated for ten cycles for all the membranes. The findings of this experiment for composite membranes containing imprinted particles are presented in Fig. 11 and compared with their corresponding non-regenerated membranes.

The outcomes clearly demonstrate that the MIP-CPES-EB can be effectively reused after undergoing the regeneration procedure, as they retain their high adsorption capacity. In all the ten adsorption cycles with regeneration, the MIP-CPES-EB membrane removed almost more than 90% of the initial E2 from water. Conversely, without undergoing the regeneration process, the adsorption capacity of the composite membrane drops considerably after the second cycle. The results were consistent with our expectations, as the regeneration procedure reactivated the adsorption properties of the particles. The regeneration procedure was also applied to the reference PES

**Fig. 12** Breakthrough curves for the reference PES and the MIP-CPES-EB membrane investigated in real water sample.

membrane (not included here). The adsorption capacity for the first cycle and the regenerated cycles was below 1%. The demonstrated reusability and the facile regeneration process for multiple adsorption/desorption cycles is a pivotal factor for the large-scale application of these composite membranes when compared to traditional adsorbent materials, which are challenging to regenerate. The regeneration process was also carried out on composite membranes containing non-imprinted particles, and the outcomes were compared with the results obtained from non-regenerated membranes (Fig. S5, ESI†).

Furthermore, the dynamic adsorption loading of the reference and MIP-CPES-EB membrane was investigated using tap water samples. An E2 solution with an initial concentration of  $5 \text{ mg L}^{-1}$  in tap-water was prepared (tap-water/ethanol (9:1, v:v)). The membranes were wetted prior to the dynamic adsorption experiments with 20 mL of tap-water/ethanol solution (9:1, v:v). 200 mL of the E2 solution in tap water was filtered through each membrane and permeate samples were taken at 20 mL intervals. The breakthrough curves are illustrated in Fig. 12. The performance of the MIP-CPES-EB membrane for the adsorption of E2 from tap water is similar to the adsorption behavior observed in E2 solutions prepared with pure water. The dynamic adsorption loading  $Q_{\text{dyn}}$  was determined to be  $12.1 \text{ mg g}^{-1}$ . The comparable adsorption loading achieved for experiments in real water suggest that the composite membranes can be practically used also in real water samples.

**Fig. 11** Adsorption capacities of the composite membranes based on 10 cycles of binding/regeneration compared to the non-regenerated composite membranes.

## Conclusion

This study describes the preparation of composite PES (CPES) membranes containing synthesized molecularly imprinted (MIP) and non-imprinted (NIP) particles for the selective and efficient removal of E2 from water. The proposed approach enables continuous water filtration while also achieving specific E2 adsorption. Compared to other adsorber membranes reported in the literature, such as NF membranes, this method represents a valuable and versatile strategy for obtaining



membranes with more than a 200-fold higher loading capacity. Furthermore, the composite membranes maintain their high-water permeability without requiring high pressure during the filtration process. The CPES membranes are also easily regenerated, demonstrating their effectiveness for sustainable processes. This study demonstrates the feasibility of integrating MIP and NIP adsorbent particles into porous polymer membranes *via* phase inversion and electron beam irradiation. Future research endeavors may explore the development of diverse functional adsorbent particles, such as those with a dual-template structure, to create tailored membranes for specific applications.

## Author contributions

Zahra Niavarani: methodology, investigation, data curation, writing – original draft, writing – review and editing. Isabell Thomas: TOC measurements. Andrea Prager: SEM and XPS measurements, Mathias Kuehnert: mercury porosimetry. Daniel Breite: writing – review and editing, supervision. Bernd Abel: writing – review and editing, supervision. Roger Gläser: writing – review and editing, supervision. Agnes Schulze: writing – review and editing, supervision.

## Conflicts of interest

There are no conflicts to declare.

## Notes and references

- 1 R. P. Schwarzenbach, B. I. Escher, K. Fenner, T. B. Hofstetter, C. A. Johnson, U. V. Gunten and B. Wehrli, The Challenge of Micropollutants in Aquatic Systems, *Science*, 2006, **313**, 1072–1077.
- 2 A. Ismanto, T. Hadibarata, R. A. Kristanti, L. Maslukah, N. Safinatunnajah and W. Kusumastuti, Endocrine disrupting chemicals (EDCs) in environmental matrices: Occurrence, fate, health impact, physio-chemical and bio-remediation technology, *Environ. Pollut.*, 2022, **302**, 119061.
- 3 M. Bilal, D. Barceló and H. M. N. Iqbal, Occurrence, environmental fate, ecological issues, and redefining of endocrine disruptive estrogens in water resources, *Sci. Total Environ.*, 2021, **800**, 149635.
- 4 Q. Che, X. Xiao, J. Xu, M. Liu, Y. Lu, S. Liu and X. Dong, 17 $\beta$ -Estradiol promotes endometrial cancer proliferation and invasion through IL-6 pathway, *Endocr. Connect.*, 2019, **8**, 961–968.
- 5 T. Wang, J. He, J. Lu, Y. Zhou, Z. Wang and Y. Zhou, Adsorptive removal of PPCPs from aqueous solution using carbon-based composites: A review, *Chin. Chem. Lett.*, 2022, **33**, 3585–3593.
- 6 F. Cecen and Ö. Aktaş, *Activated Carbon for Water and Wastewater Treatment: Integration of Adsorption and Biological Treatment*, Wiley-VCH Verlag GmbH & Co. KGaA, 2011.
- 7 E. Gagliano, M. Sgroi, P. P. Falciglia, F. G. A. Vagliasindi and P. Roccaro, Removal of poly- and perfluoroalkyl substances (PFAS) from water by adsorption: Role of PFAS chain length, effect of organic matter and challenges in adsorbent regeneration, *Water Res.*, 2020, **171**, 115381.
- 8 P. Márquez, A. Benítez, A. F. Chica, M. A. Martín and A. Caballero, Evaluating the thermal regeneration process of massively generated granular activated carbons for their reuse in wastewater treatments plants, *J. Cleaner Prod.*, 2022, **366**, 132685.
- 9 M. Zambianchi, M. Durso, A. Liscio, E. Treossi, C. Bettini, M. L. Capobianco, A. Aluigi, A. Kovtun, G. Ruani, F. Corticelli, M. Brucale, V. Palermo, M. L. Navacchia and M. Melucci, Graphene oxide doped polysulfone membrane adsorbers for the removal of organic contaminants from water, *Chem. Eng. J.*, 2017, **326**, 130–140.
- 10 L.-h. Jiang, Y.-g. Liu, G.-m. Zeng, F.-y. Xiao, X.-j. Hu, X. Hu, H. Wang, T.-t. Li, L. Zhou and X.-f. Tan, Removal of 17 $\beta$ -estradiol by few-layered graphene oxide nanosheets from aqueous solutions: External influence and adsorption mechanism, *Chem. Eng. J.*, 2016, **284**, 93–102.
- 11 J. J. BelBruno, Molecularly Imprinted Polymers, *Chem. Rev.*, 2019, **119**, 94–119.
- 12 Z. Zhongbo and J. Hu, Selective removal of estrogenic compounds by molecular imprinted polymer (MIP), *Water Res.*, 2008, **42**, 4101–4108.
- 13 Y. Lin, Y. Shi, M. Jiang, Y. Jin, Y. Peng, B. Lu and K. Dai, Removal of phenolic estrogen pollutants from different sources of water using molecularly imprinted polymeric microspheres, *Environ. Pollut.*, 2008, **153**, 483–491.
- 14 L. P. d Santos Xavier, A. C. Dias, B. E. L. Baeta, L. de Azevedo Santos, T. C. Ramalho, S. F. de Aquino and A. C. da Silva, Experimental and theoretical studies of solvent polarity influence on the preparation of molecularly imprinted polymers for the removal of estradiol from water, *New J. Chem.*, 2019, **43**, 1775–1784.
- 15 H. Li, Y. Liu, Z. Zhang, H. Liao, L. Nie and S. Yao, Separation and purification of chlorogenic acid by molecularly imprinted polymer monolithic stationary phase, *J. Chromatogr. A*, 2005, **1098**, 66–74.
- 16 K. Niedergall, M. Bach, T. Schiestel and G. E. M. Tovar, Nanostructured Composite Adsorber Membranes for the Reduction of Trace Substances in Water: The Example of Bisphenol A, *Ind. Eng. Chem. Res.*, 2013, **52**, 14011–14018.
- 17 C. Gkementzoglou, O. Kotrotsiou, M. Koronaiou and C. Kiparissides, Development of a sandwich-type filtration unit packed with MIP nanoparticles for removal of atrazine from water sources, *Chem. Eng. J.*, 2016, **287**, 233–240.
- 18 A. Schulze, B. Marquardt, S. Kaczmarek, R. Schubert, A. Prager and M. R. Buchmeiser, Electron Beam-Based Functionalization of Poly(ethersulfone) Membranes, *Macromol. Rapid Commun.*, 2010, **31**, 467–472.
- 19 M. Schmidt, S. Zahn, F. Gehlhaar, A. Prager, J. Griebel, A. Kahnt, W. Knolle, R. Konieczny, R. Gläser and A. Schulze, Radiation-Induced Graft Immobilization (RIGI): Covalent Binding of Non-Vinyl Compounds on Polymer Membranes, *Polymers*, 2021, **13**(11), 1849.



- 20 B. Van der Bruggen, Chemical modification of polyether-sulfone nanofiltration membranes: A review, *J. Appl. Polym. Sci.*, 2009, **114**, 630–642.
- 21 R. Das, M. Kuehnert, A. Sadat Kazemi, Y. Abdi and A. Schulze, Water Softening Using a Light-Responsive, Spiropyran-Modified Nanofiltration Membrane, *Polymers*, 2019, **11**, 344.
- 22 M. D. Celiz, D. S. Aga and L. A. Colón, Evaluation of a molecularly imprinted polymer for the isolation/enrichment of  $\beta$ -estradiol, *Microchem. J.*, 2009, **92**, 174–179.
- 23 W.-H. Li and H. D. H. Stöver, Porous monodisperse poly(divinylbenzene) microspheres by precipitation polymerization, *J. Polym. Sci., Part A: Polym. Chem.*, 1998, **36**, 1543–1551.
- 24 A. M. Comerton, R. C. Andrews, D. M. Bagley and P. Yang, Membrane adsorption of endocrine disrupting compounds and pharmaceutically active compounds, *J. Membr. Sci.*, 2007, **303**, 267–277.
- 25 J. W. Kwon and K. L. Armbrust, Aqueous Solubility, n-Octanol–Water Partition Coefficient, and Sorption of Five Selective Serotonin Reuptake Inhibitors to Sediments and Soils, *Bull. Environ. Contam. Toxicol.*, 2008, **81**, 128–135.
- 26 D. Breite, M. Went, I. Thomas, A. Prager and A. Schulze, Particle adsorption on a polyether sulfone membrane: how electrostatic interactions dominate membrane fouling, *RSC Adv.*, 2016, **6**, 65383–65391.
- 27 Z. Niavarani, D. Breite, A. Prager, B. Abel and A. Schulze, Estradiol Removal by Adsorptive Coating of a Microfiltration Membrane, *Membranes*, 2021, **11**(2), 99.
- 28 A. J. C. Semião and A. I. Schäfer, Estrogenic micropollutant adsorption dynamics onto nanofiltration membranes, *J. Membr. Sci.*, 2011, **381**, 132–141.
- 29 L. Ye and K. Mosbach, Molecularly imprinted microspheres as antibody binding mimics, *React. Funct. Polym.*, 2001, **48**, 149–157.
- 30 B. Sellergren, Polymer- and template-related factors influencing the efficiency in molecularly imprinted solid-phase extractions, *TrAC, Trends Anal. Chem.*, 1999, **18**, 164–174.
- 31 S. Wei, A. Molinelli and B. Mizaikoff, Molecularly imprinted micro and nanospheres for the selective recognition of 17 $\beta$ -estradiol, *Biosens. Bioelectron.*, 2006, **21**, 1943–1951.
- 32 T. Fukuhara, S. Iwasaki, M. Kawashima, O. Shinohara and I. Abe, Adsorbability of estrone and 17 $\beta$ -estradiol in water onto activated carbon, *Water Res.*, 2006, **40**, 241–248.
- 33 L. T. Son, K. Katagawa and T. Kobayashi, Using molecularly imprinted polymeric spheres for hybrid membranes with selective adsorption of bisphenol A derivatives, *J. Membr. Sci.*, 2011, **375**, 295–303.
- 34 A. Schulze, M. F. Maitz, R. Zimmermann, B. Marquardt, M. Fischer, C. Werner, M. Went and I. Thomas, Permanent surface modification by electron-beam-induced grafting of hydrophilic polymers to PVDF membranes, *RSC Adv.*, 2013, **3**, 22518–22526.
- 35 İ. Koç, G. Baydemir, E. Bayram, H. Yavuz and A. Denizli, Selective removal of 17 $\beta$ -estradiol with molecularly imprinted particle-embedded cryogel systems, *J. Hazard. Mater.*, 2011, **192**, 1819–1826.
- 36 E. A. McCallum, H. Hyung, T. A. Do, C.-H. Huang and J.-H. Kim, Adsorption, desorption, and steady-state removal of 17 $\beta$ -estradiol by nanofiltration membranes, *J. Membr. Sci.*, 2008, **319**, 38–43.
- 37 Y.-M. Ren, J. Yang, W.-Q. Ma, J. Ma, J. Feng and X.-L. Liu, The selective binding character of a molecular imprinted particle for Bisphenol A from water, *Water Res.*, 2014, **50**, 90–100.
- 38 K. Niedergall, M. Bach, T. Hirth, G. E. M. Tovar and T. Schiestel, Removal of micropollutants from water by nanocomposite membrane adsorbers, *Sep. Purif. Technol.*, 2014, **131**, 60–68.

